ELSEVIER

Journal of Hazardous Materials 62 (1998) 243–264

JOURNAL OF HAZARDOUS MATERIALS

# Reductive dehalogenation of trichloroethylene: kinetic models and experimental verification

Jayant K. Gotpagar, Eric A. Grulke, Dibakar Bhattacharyya *

*Department of Chemical and Materials Engineering, University of Kentucky, Lexington, KY 40506-0046, USA*

Received 2 February 1998; revised 7 July 1998; accepted 8 July 1998

**Abstract**

This paper develops a generalized kinetic model for two-phase systems involving reactions in one phase with product partitioning into a second phase, and applies it to the reductive dehalogenation of trichloroethylene using two systems. The generalized approach can be used for a variety of catalyst choices, including zero-valent metals. With vitamin $B_{12}$, the model includes specific reaction pathways for the reductive dehalogenation of TCE combined with the partitioning of reactants, intermediates, and products between the gas and liquid phases. The model has been used to study the effect of various parameters on the process effectiveness, which otherwise are very difficult to conceive through experimental analysis. In the case of zero-headspace system with zero-valent iron, sorption effects are included to incorporate the partitioning onto the solid surface. A new parameter, 'fractional active site concentration' is introduced to incorporate the differences in reactive and nonreactive sites on the iron surface, which affects the degradation performance. The generalized model has important implications for kinetic modeling, monitoring of VOCs and their degradation products, and design and selection of remediation technologies for such materials. The model predictions have been verified with our experimental data and the results from the literature. 

*Keywords:* Trichloroethylene; Kinetic; Iron; Vitamin $B_{12}$; Sorption; Model; Dehalogenation

## 1. Introduction

Remediation of trichloroethylene (TCE) contaminated soils and groundwater is an issue of importance because of the potentially carcinogenic nature of TCE (and the products of degradation), and its resistance to natural attenuation in the environment.

* Corresponding author. Tel.: +1 606 257 2794; fax: +1 606 323 1929; e-mail: db@engr.uky.edu

0304-3894/98/$ - see front matter 
PII: S0304-3894(98)00184-8

Conventional wastewater treatment processes are unable to bring down the TCE levels to drinking water standard (5 ppb) [40 CFR, Part 141]. Various ex-situ processes like activated carbon adsorption [1] and air stripping [2] are effective in achieving drinking water standards, but in these, the contaminant still must be removed from the solid or vapor medium. The use of advanced oxidation processes such as $UV/O_3/H_2O_2$ has also been reported in the literature [3]. These processes are limited to ex-situ treatment.

For in-situ treatment, one of the emerging technologies is reductive dehalogenation using zero-valent metals. Various metals such as Fe, Sn, and Zn have been found effective in degrading halogenated hydrocarbons, and the rates of these processes are much faster compared to those of biodegradation or natural attenuation [4–11]. At room temperature, the degradation is faster than the natural attenuation, but still can take days when zero-valent iron is used. In case of trichloroethylene, the mechanism involved is believed to be direct electrolytic reduction at the metal surface [12]. Researchers have identified different metals for the process, but have paid little attention to the kinetics of reductive dehalogenation. The mechanism and product distribution for reductive dehalogenation varies for different metals and catalysts [5] and often includes very low rates of decomposition for volatile intermediates. The rate of degradation of intermediate species is slower than that of TCE. The design of monitoring and remediation systems for groundwater contaminated with TCE would require detailed kinetic analysis of the degradation since most of the possible products have highly stringent regulations.

## 2. Reaction mechanism and product distribution

Several researchers have studied the reductive dehalogenation of trichloroethylene using different systems. Various mechanisms have been proposed. TCE appears to degrade via a pseudo-first order process. Matheson and Tratnyek [12] suggest that electrons transfer to TCE to form ethene as the primary product. Others have observed incomplete dechlorination [13,14]. Gillham and O'Hannesin [15] observed less than 10% of the parent TCE in terms of various intermediates at the end of the reaction. Not all intermediates (*cis*-1,2-DCE in particular) appear to degrade completely over the same time scale as TCE. Roberts et al. [16], have shown that over 150 h, though most of *trans*-1,2-DCE gets degraded, *cis*-1,2-DCE remains persistent. They observed complete dechlorination of *trans*-1,2-DCE, but found only 65–70% degradation of the *cis*-1,2-DCE. The *cis*-1,2-DCE concentration profile vs. time appeared to reach a limiting value.

Vitamin $B_{12}$ has also been found to be effective in reductively dehalogenating TCE [14,15,17,18]. In the presence of a bulk electron donor like titanium (III) citrate, nucleophilic substitution is generally thought to be the initial step. Mechanistic aspects of the degradation of various intermediate chlorocarbon compounds using vitamin $B_{12}$ is discussed by Glod et al. [19]. Complete material balances are reported by Burris et al. [14] for the reductive dehalogenation of TCE using vitamin $B_{12}$. The reduction is believed to occur via Co(I) center of vitamin $B_{12}$, which acts as a strong nucleophile in the presence of titanium (III) citrate. Their results also show the persistence of *cis*-1,2-DCE isomer at long reaction times (300 h), suggesting an apparent incomplete dechlorination. A kinetic analysis of their data is possible because all the intermediates

have been reported, and the effects of their partitioning into the gas phase can be evaluated. The general principles used for the vitamin $B_{12}$ case should apply to other cases in which the catalyst or reactive agent only appears in the liquid phase. There is a need to develop a model which predicts the concentration profiles of different reactants and intermediates in both phases.

The following discussion focuses on the principles used in development of a generalized model.

## 3. Theory: generalized model development

In this section, the theory and principles used for two-phase modeling are described briefly. In the subsequent sections, the guidelines developed here are applied to the case study of trichloroethylene reductive dehalogenation using two different systems.

Consider a series of irreversible reactions taking place in a closed, two-phase system. The phases involved are aqueous phase and gas phase. The reaction sequence consists of both series and parallel reactions. In a simple case, a volatile reactant A undergoes irreversible reactions in series and parallel manner to give rise to volatile products B and C, respectively. The intermediate product B may also undergo irreversible reaction to give final product D. This simple scheme can thus be represented as:

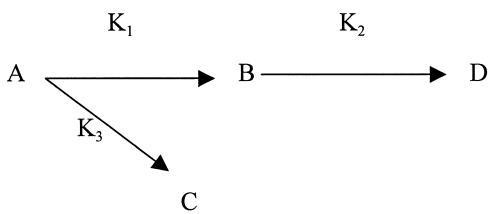


These species will be present in both aqueous and gaseous phase, the respective amount depends on their volatility. Furthermore, the volatility depends on the magnitude of the Henry's law constant, which is the measure of the air–water partitioning. Thus, the concentrations of each of these species change in both the phases because of the combined effect of reaction and partitioning. If we further assume that the reaction is taking place only in aqueous phase, then the changes in gas phase will be entirely due to the mass transfer of species under the driving force of the concentration gradient created by the reaction in the aqueous phase. A set of differential equations for each component needs to be solved simultaneously in order to describe such a system completely. Note that, due to presence of two phases, we need such equations separately for each phase, in the absence of any constraint. With this particular example, the equations can be given as follows:

$$-\frac{V_W \mathrm{d}C_A^w}{\mathrm{d}t} = k_1\left(C_A^w\right)^1 V_w + k_3\left(C_A^w\right)^m V_w - \left(k_{g,A}a\right)V_w\left(C_A^g - K_{H,A}\frac{C_A^w}{RT}\right) \quad (1)$$

$$-\frac{V_W \mathrm{d}C_B^w}{\mathrm{d}t} = -k_1\left(C_A^w\right)^1 V_w + k_2\left(C_B^w\right)^n V_w + \left(k_{g,B}a\right)V_w\left(C_B^g - K_{H,B}\frac{C_B^w}{RT}\right) \quad (2)$$

and:

$$-\frac{V_W \mathrm{d}C_C^w}{\mathrm{d}t} = -k_3\left(C_A^w\right)^m V_w + \left(k_{g,B}a\right)V_w\left(C_B^g - K_{H,B}\frac{C_B^w}{RT}\right) \quad (3)$$

where $l$, $m$, and $n$ are the orders of respective irreversible reactions. $k_{g,i}$ and $K_{H,i}$ are the mass transfer coefficients (m/h) and dimensionless Henry's law constants for compound $i$. The superscript w and g refer to the aqueous and gas phase, respectively. $a$ is the interfacial surface area (gas/liquid interface) per unit volume of the solution.

As noted earlier, these differential equations need to be solved simultaneously (with proper initial conditions), to get the temporal profile of all the compounds. In the simplest case, when $l$, $m$ and, $n$ are all equal to 1, i.e. the first order reaction sequence, the analytical solution is straightforward and we can easily get the concentration profiles. However, in the cases where analytical solutions do not exist, these equations can be solved numerically (if the mass transfer constants and rate constants are known or can be estimated) to get the desired profiles. If the exact reaction sequence is known, and the experimental data for all the product distribution is available, then such model can also be used to evaluate the values of intrinsic rate constants of individual steps. The reaction sequence can thus be delineated easily which otherwise could be very difficult to achieve through trial and error experimental approach. With the help of this model, we can also study the relative importance of different steps governing the system and arrive at the rate-limiting step. Finally, such a model can be used to study the effect of different physical variables on the performance of the system and optimum conditions for design could be achieved.

In the subsequent sections, we apply this model to the reductive dehalogenation of trichloroethylene using two examples reported in the literature. Using these examples, it is shown how such a model can be used to arrive at the intrinsic rate constants, delineate different steps and find out the rate-limiting step. The model developed is also used to simulate the effect of various physical variables on the system performance.

## 4. Example 1: trichloroethylene reduction using vitamin $B_{12}$

This section describes the application of the model for the degradation of trichloroethylene using vitamin $B_{12}$. Fig. 1 summarizes the reaction products proposed for TCE by several researchers. Burris et al. [14] used excess of titanium citrate as the

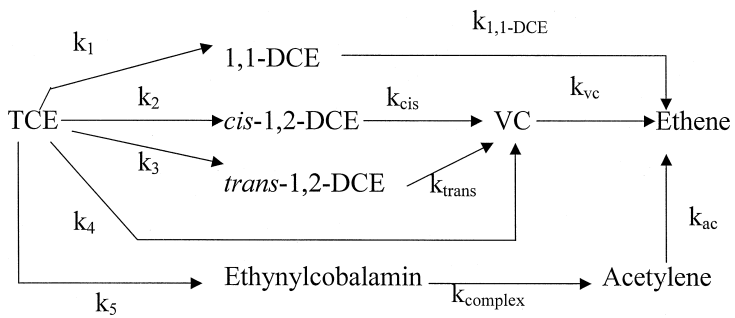


Fig. 1. Proposed reaction scheme for reductive dehalogenation of trichloroethylene using vitamin $B_{12}$.

reductant, resulting in pseudo-first order behavior for TCE reduction by vitamin $B_{12}$. In the recently published study [19], it has been shown that, in the case of most of these chlorocarbon compounds, the first step of degradation involves the formation of the alkylcobalamin complex, which further degrades to give daughter products. For the purpose of this model, it is assumed that the reactions proceed via first order process with respect to the parent compound; the effect of vitamin $B_{12}$ and pH is not considered. However, both these effects can be readily incorporated in the model. The only complex considered in this particular exercise is Ethynylcobalamin, the intermediate complex formed between TCE and vitamin $B_{12}$. Semadeni et al. [18] observed that some portion of TCE undergoes reductive β-elimination to yield chloroacetylene that can further yield acetylene or vinyl chloride. The chloroacetylene was found to degrade very rapidly (because of its unstable nature). Vinyl chloride was formed as long as there was free chloroacetylene in the system and that conversion was believed to occur through free radical (dichlorovinyl) intermediate. Because of such unstable nature of chloroacetylene, in this modeling exercise, vinyl chloride is assumed to form directly from TCE. Acetylene on the other hand was thought to be formed through an intermediate complex, Ethynylcobalamin. The behavior of all the other compounds can also be included in the similar way. Acetylene formation observed in the study was attributed to the reductive β-elimination mechanism. This was confirmed by Semadeni et al. [18], who have reported the reductive transformation of chlorinated ethenes using vitamin $B_{12}$. This group of researchers also studied the degradation of *cis*-1,2-DCE and *trans*-1,2-DCE isomers. They found that both these isomers degrade slowly to vinyl chloride, the only observed product. In case of 1,1-DCE however, ethene was found to be the main product. Based on all these experimental observations, the following assumptions were made.

### *4.1. Model assumptions (specific to a vitamin $B_{12}$ catalyst)*

1. Reactions are assumed to be irreversible.
2. All the reactions are considered to be first order with respect to the starting compound.
3. The liquid and gas phases are isothermal and well mixed.
4. Chlorocarbon degradation reactions take place only in aqueous phase and not at the gas/liquid interface.
5. *cis*-1,2-DCE and *trans*-1,2-DCE degrade to give vinyl chloride as the major product.
6. Some of the vinyl chloride is formed directly from TCE because of the unstable chloroacetylene intermediate.
7. Acetylene is formed from the TCE through intermediate complex Ethynylcobalamin.
8. 1,1-DCE is assumed to degrade slowly to ethene.
9. Mass transfer coefficients for all the DCE isomers are assumed to be the same.
10. Formation of acetylene from 1,1-DCE, *cis*-1,2-DCE and *trans*-1,2-DCE is neglected.

Based on these assumptions, the reaction scheme for TCE reduction using vitamin $B_{12}$ is shown in Fig. 1.

All the compounds under consideration are highly volatile, and owing to their low solubilities in aqueous phase, the intermediate species will tend to partition into headspace (if present), as they are formed. The reaction system is closed and well-mixed, and no apparent losses to the surroundings are assumed. We assumed that the mass transfer coefficients of various compounds can be related to the 0.6 power of their ratio of molecular weights [20], and that only one mass transfer coefficient is needed to characterize the entire set of halocarbon coefficients. For example:

$$K_a = K_b \times \left( \frac{M_a}{M_b} \right)^{0.6} \tag{4}$$

where $K_a$ and $K_b$ are the mass transfer coefficients and $M_a$ and $M_b$ are molecular weights of compounds A and B, respectively.

### *4.2. Aqueous phase balance*

All the reactions occur in the aqueous phase. Based on these assumptions and reactions sequence, we can write the component balance for each compound in aqueous phase and gaseous phase. The symbol $C_i^j$ refers to the concentration of a compound $i$. The superscript $j$ refers to the phase. The mass balance equations in the aqueous phase can be written as:

$$-\frac{dC_i^w}{dt} = -\sum k_{formation} C_j^w + \sum k_{degradation} C_i^w + \text{mass transfer term} \tag{5}$$

where the first term gives the rate of formation of species $i$ from all routes and, the second term gives the total disappearance rate of the compound $i$ into its possible daughter products. The mass transfer term accounts for the transfer of species from gas to liquid (and vice versa) for each component and is given by:

$$\text{mass transfer term} = k_{g,i} a \left( C_i^g - K_{H,i} C_i^w \right) \tag{6}$$

where, $k_{g,i}$ is the mass transfer coefficient for component $i$ (m/h) and, $a$ is the interfacial surface area (gas/liquid) per unit volume of the solution ($m^{-1}$). $K_{H,i}$ is the dimensionless Henry's law constant for compound $i$.

For example, balance for trichloroethylene in the aqueous phase can be written as:

$$-\frac{V_W dC_{TCE}^w}{dt} = k_{TCE} C_{TCE}^w V_w - \left( k_{g,TCE} a \right) V_w \left( C_{TCE}^g - K_{H,TCE} C_{TCE}^w \right) \tag{7}$$

and that for 1,1-DCE is:

$$-\frac{V_w dC_{1,1\text{-DCE}}^w}{dt} = k_{1,1\text{-DCE}} C_{1,1\text{-DCE}}^w V_w - k_{\text{TCE-}1,1\text{-DCE}} C_{TCE}^w V_w - \left( k_{g,DCE} a \right) V_w \times \left( C_{1,1\text{-DCE}}^g - K_{H,1,1\text{-DCE}} C_{1,1\text{-DCE}}^w \right) \tag{8}$$

Similarly, the balances can be written for all the other compounds in terms of their formation and degradation rate constants and mass transfer coefficients.

### 4.3. Mass balances in the gas phase

As there is no reaction in the gas phase, the concentration changes occur only by mass transfer. Hence the generalized mass balance in the gas phase can be written as follows:

$$-\frac{V_g \mathrm{d}C_i^g}{\mathrm{d}t} = (k_{g,i}a)V_w(C_i^g - K_{H,i}C_i^w) \tag{9}$$

The balance is written for all the species.

### 4.4. Initial conditions

We have verified the model using the study reported in the literature [14]. In this, the reductions were carried out in 0.160 l serum vials, sealed with Teflon lined septa. The batch systems included 0.1 l of aqueous phase and 0.06 l of headspace. Thus, the ratio $V_g/V_w$ was 0.6 for the experimental setup. The vial contained vitamin $B_{12}$ at a concentration of 10 μM. Around 16.6 μmol of TCE in 400 μg of pentane was then spiked into each vial and was allowed to partition between the gas and water phases. Titanium (III) citrate was injected into the aqueous phase (15 mM concentration) to initiate the reaction. The initial conditions were:

$$\begin{aligned}
&C_{TCE}^w(0) = C_0\\
&C_{TCE}^g(0) = K_{H,TCE}C_0\\
&C_{1,1\text{-DCE}}^w(0) = C_{cis\text{-DCE}}^w(0) = C_{trans\text{-DCE}}^w(0) = C_{VC}^w(0) = C_{AC}^w(0) = C_{ET}^w(0) = 0\\
&C_{1,1\text{-DCE}}^g(0) = C_{cis\text{-DCE}}^g(0) = C_{trans\text{-DCE}}^g(0) = C_{VC}^g() = C_{AC}^g(0) = C_{ET}^g(0) = 0
\end{aligned} \tag{10}$$

### 4.5. Results and discussion

A set of Eqs. (5) and (9) can be solved simultaneously using the initial conditions, Eq. (10), to predict the component distributions with time. The unknowns under considerations are the individual rate constants, and one mass transfer coefficient. A compendium of partition coefficients for different chlorocarbon compounds is given in literature [21,22]. Different studies report a range of Henry's law constants for these species, and often there is wide variation between the reported values for the same compound. We have made use of the experimentally observed Henry's law constants in this study. A commonly used experimental method for measuring air–water partitioning for volatile compounds is so called EPICS (Equilibrium Partitioning In Close System) method. Gossett [23] has reported the measured Henry's law constants for different chlorinated hydrocarbons. Summary of these dimensionless constants is shown in Table 1. These values were used during model simulation. The Laplace Transform method

Table 1
Henry's law constants for TCE, DCE isomers and vinyl chloride between air and water [23]

| Chlorocarbon compound | $K_H$ (dimensionless) |
|---|---|
| *trans*-DCE | 0.3011 |
| *cis*-DCE | 0.1216 |
| 1,1-DCE | 0.8586 |
| TCE | 0.2964 |
| Vinyl chloride | 0.9014 |

(Maple V software package, Release 4, Version 4.00, Waterloo Maple) was used to get the analytical expressions in time for each component. The objective function to be minimized was the sum of the squares of errors between the experimental and predicted values for each of the species at different times. The selected value of the rate constant and/or mass transfer coefficient was that which minimized this objective function. We have modeled the total molar values of each component in the reaction system (gas + aqueous phase).

As the reactions under consideration are very slow (half lives ranging in days), it is quite possible that the mass transfer can be in equilibrium compared to the reaction in the liquid phase. To check this hypothesis, only TCE equations were first solved to get the rate constant and mass transfer coefficient value for this compound. It can be seen from Eq. (4) that the mass transfer coefficients for intermediate halocarbon compounds would be lower than that TCE. Furthermore, as mentioned earlier, the rates of degradation of these intermediate species are slower than TCE. Hence, it is conservative to use only TCE balance to check for the hypothesis of gas–liquid equilibrium.

TCE degradation depends only on the degradation rate constant and the mass transfer coefficient. Fig. 2 shows that the model fits the data of Ref. [14] accurately over its entire range. The calculated values of the degradation rate constant and mass transfer coefficient values are:

$$k_{\mathrm{TCE}} = 0.0217/\mathrm{h}$$
$$k_{\mathrm{g,TCE}}\, a = 2.698/\mathrm{h}$$

Thus, the mass transfer rate of TCE to the liquid phase is indeed almost two orders of magnitude higher than the degradation rate for TCE in the aqueous phase. If the rate of reaction is comparable to the rate of mass transfer, these coefficients would be highly coupled, and we would need to determine the mass transfer coefficients for all components simultaneously with the appropriate rate constants. Based on this result, we simplified the analysis further by neglecting the mass transfer flux, and assuming rapid equilibrium. This leaves only one set of unknown concentrations—those of the aqueous phase. Gaseous phase concentrations can be computed from these using partition coefficients. The generalized balance for aqueous phase concentrations with rapid equilibrium is:

$$-\left(1 + K_{\mathrm{H},i}\frac{V_{\mathrm{g}}}{V_{\mathrm{w}}}\right)\frac{\mathrm{d}C_i^{\mathrm{w}}}{\mathrm{d}t} = -\Sigma k_{\mathrm{formation}} C_j^{\mathrm{w}} + \Sigma k_{\mathrm{degradation}} C_i^{\mathrm{w}} \qquad (11)$$

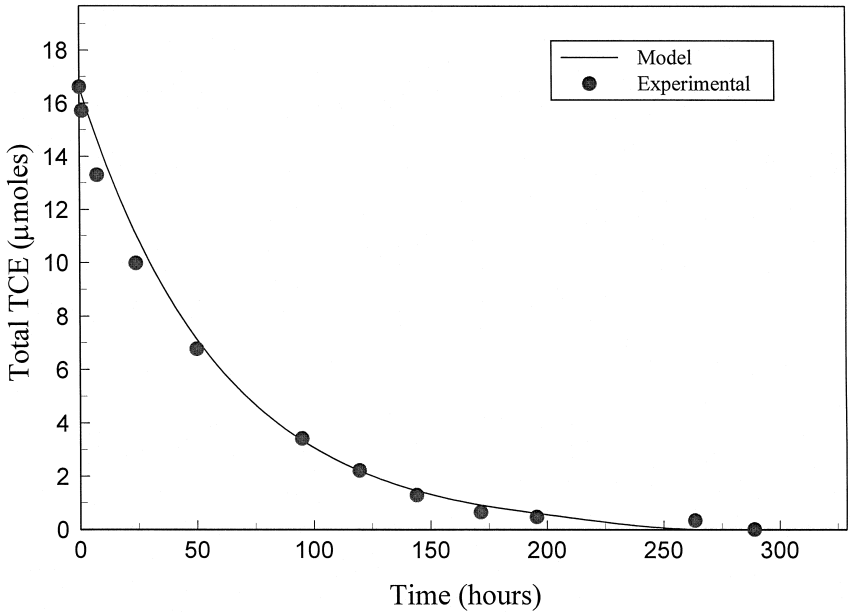


Fig. 2. Reductive dehalogenation of TCE by vitamin $B_{12}$ in homogeneous solution. Symbols: experimental data [14]. Line: prediction of model considering liquid–gas mass transfer effect.

Thus, we are left with a system of linear differential equations with constant coefficients. These can be solved easily by an analytical method using integration factors to get the product profiles in terms of unknown constants $k$s, from which the model parameters can be determined. For example, the analytical expression for a DCE isomer is:

$$C_{\mathrm{D}i}^{\mathrm{w}} = \frac{k_{\mathrm{TCE-D}i} C_0}{\left(1 + K_{\mathrm{H},i}\dfrac{V_{\mathrm{g}}}{V_{\mathrm{w}}}\right)\left(k_{\mathrm{D}i}^{\mathrm{app}} - k_{\mathrm{TCE}}^{\mathrm{app}}\right)}\left[\exp\left(-k_{\mathrm{TCE}}^{\mathrm{app}} t\right) - \exp\left(-k_{\mathrm{D}i}^{\mathrm{app}} t\right)\right] \tag{12}$$

where $C_{\mathrm{D}i}^{\mathrm{w}}$ is the aqueous phase concentration of DCE isomer $i$ ($i$ stands for 1,1-DCE, *cis*-1,2-DCE or *trans*-1,2-DCE). $k_i^{\mathrm{app}}$ is the apparent degradation constant of specie $i$ due to partitioning effect and is related to the intrinsic rate constant by following equation:

$$k_i^{\mathrm{app}} = \frac{k_i}{\left(1 + K_{\mathrm{H},i}\left(\dfrac{V_{\mathrm{g}}}{V_{\mathrm{w}}}\right)\right)} \tag{13}$$

*4.5.1. Reaction rate constants*

Twelve reaction rate constants are needed (Fig. 1). These include seven degradation rate constants, $k_{\mathrm{TCE}}$, $k_{1,1\text{-DCE}}$, $k_{cis\text{-DCE}}$, $k_{trans\text{-DCE}}$, $k_{\mathrm{VC}}$, $k_{\mathrm{AC}}$, $k_{\mathrm{complex}}$, and five forma-

tion rate constants, $k_{\text{TCE-1,1-DCE}}$, $k_{\text{TCE-}cis\text{-DCE}}$, $k_{\text{TCE-}trans\text{-DCE}}$, $k_{\text{TCE-VC}}$, and $k_{\text{TCE-complex}}$. We have one constraint on the formation rate constants: their sum has to equal the total degradation rate constant for TCE. Thus:

$$k_{\text{TCE}} = k_{\text{TCE-1,1-DCE}} + k_{\text{TCE-}cis\text{-DCE}} + k_{\text{TCE-}trans\text{-DCE}} + k_{\text{TCE-VC}} + k_{\text{TCE-complex}} \tag{14}$$

The summary of the rate constants used to fit the model to the data is given in Table 2.

The value obtained for TCE degradation constant ($0.0217\ \text{h}^{-1}$), is in good agreement with the published data [14,18]. We have done experimental studies on TCE reduction using zero-valent iron in zero-headspace system [13]. Interestingly, the value of rate constant was also found to be in close agreement with our iron studies. Among the DCE isomers, 1,1-DCE was found to have the highest degradation constant, which is also consistent with the findings of Glod et al. [19]. Fig. 3a and b show that with the exception of 1,1-DCE, the model fits the experimental data accurately over the entire time range for TCE, *cis*-DCE, *trans*-DCE, vinyl chloride, acetylene and ethene. In case of 1,1-DCE however, there is deviation from the data at short times, with the model predicted concentrations lower than the measured values. The rate constants used to fit the data (Table 2), are the set of constants that best fit the experimental data for all the intermediates. The experimental data show around 20% unaccounted carbon at long times. This suggests that there may be unknown pathways that need to be considered in order to completely model the system. Descriptions of some of these are given by Glod et al. [17,19], who studied the mechanistic aspects of the reaction. We have accounted for one of these in the model by considering the complex formation (Fig. 1). This complex would not be detected by the analytical method used. Nonetheless, it does show one of the existing pathways. In the similar manner, there exist other $B_{12s}$–substrate complexes, which we have not accounted for [19]. This further, can cause deviation from the first order approximation used in this study. These might be some of the reasons for difference between model predictions and experimental observation for 1,1-DCE. We are currently in the process of relaxing these assumptions.

In systems like these, where the compounds involved pose lot of analytical difficulties, it is often very difficult to achieve complete material balance. This experimental

Table 2
Summary of rate constants used in Example 1

| Chlorocarbon compound | Intrinsic rate constant $k \times 10^5$ ($\text{h}^{-1}$) |
|---|---|
| TCE | $k^{\text{a}}_{\text{TCE}} = 2172.1$ |
| 1,1-DCE | $k_{\text{1,1-DCE}} = 779.4$ |
| *cis*-DCE | $k_{cis} = 1.2$ |
| *trans*-DCE | $k_{trans} = 78.9$ |
| Vinyl chloride | $k_{\text{VC}} = 69.21$ |
| Acetylene | $k_{\text{AC}} = 885$ |
| Ethynylcobalamin complex | $k_{\text{complex}} = 1130$ |

[a] $k_{\text{TCE}} = k_{\text{TCE-1,1-DCE}} + k_{\text{TCE-}cis\text{-DCE}} + k_{\text{TCE-}trans\text{-DCE}} + k_{\text{TCE-VC}} + k_{\text{TCE-complex}}$
$= 1.35\times10^{-4} + 1.17\times10^{-2} + 4.76\times10^{-4} + 6.51\times10^{-5} + 9.33\times10^{-3}$.

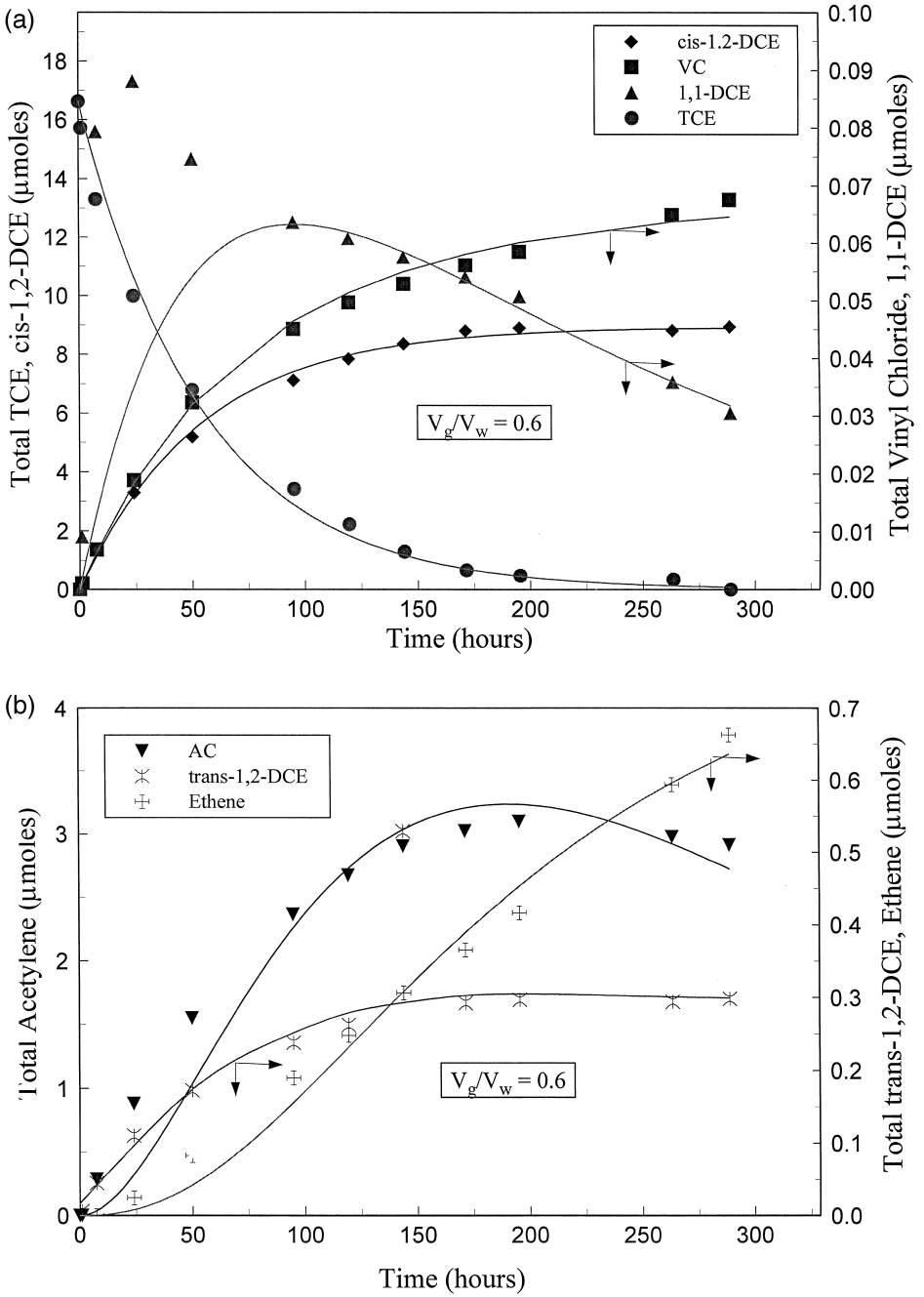


Fig. 3. Product distribution in the case of reductive dehalogenation of TCE by vitamin $B_{12}$ in homogeneous solution. (a) *cis*-1,2-DCE, VC, 1,1-DCE, TCE, (b) AC, *trans*-1,2-DCE, and ethene. Symbols: experimental data [14]. Lines: prediction of model assuming pseudo-equilibrium between liquid and gas phase.

problem further hinders the delineation of different steps involved, and sound knowledge of the governing intrinsic constants which are crucial in design of a remediation system. Following subsections illustrate how such a model can be used to study the system behavior with variation of different important physical parameters, which can further shed some light on the future research directions required to achieve the efficient performance.

*4.5.2. Model sensitivity to phase equilibria*

Varying two different parameters can simulate the partitioning effect: Henry's law constant, $K_H$ and the ratio of headspace volume to aqueous phase volume ($V_g/V_w$).

*4.5.2.1. Effect of $V_g/V_w$ ratio.* Fig. 4 illustrates the effect of $V_g/V_w$ ratio on the simulated TCE degradation and ethene production. As can be seen from the figure, low $V_g/V_w$ values have insignificant effect on the overall TCE degradation rate. If the gas to liquid ratio increases, more TCE migrates to the gas phase and the degradation rate decreases considerably. Similar effect is observed on the ethene formation. At low $V_g/V_w$ values, ethene formation increases. Thus, even though TCE degradation is not affected much by the $V_g/V_w$ ratio at low $V_g/V_w$ values, ethene production shows considerable effect. This can be explained based on the volatilities of different compounds involved. Vinyl chloride, 1,1-DCE and acetylene which are the precursors of ethene, have much higher Henry's law constants than TCE. Consequently, lowering the headspace will restrict these compounds to remain in the aqueous phase yielding more ethene production.

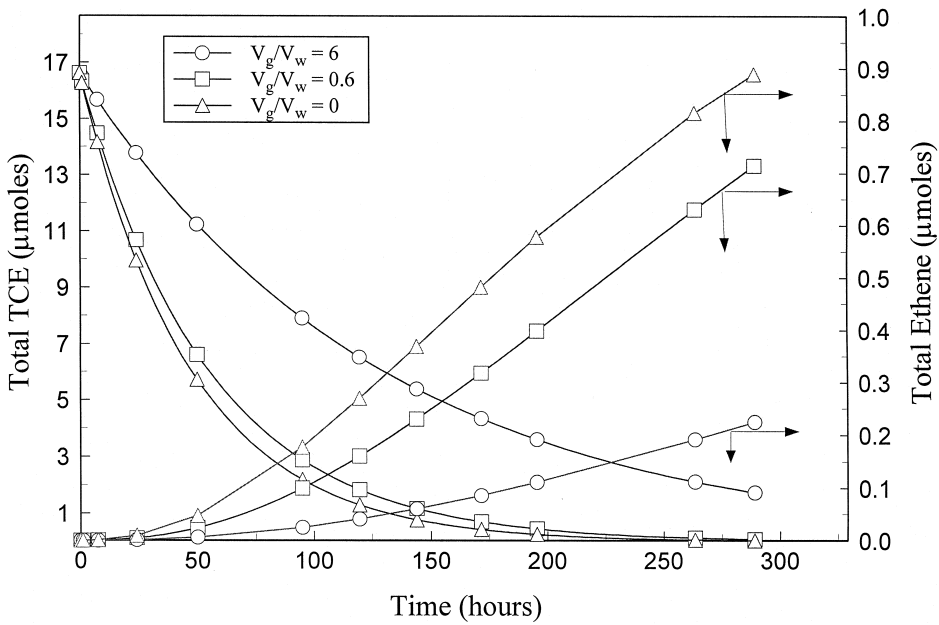


Fig. 4. Effect of $V_g/V_w$ ratio on simulated TCE degradation and ethene production in case of reductive dehalogenation of TCE using vitamin $B_{12}$.

*4.5.2.2. Effect of $K_H$.* The variation of Henry's law constants also revealed the similar results (not shown). The Henry's law constant was varied over two orders of magnitude on either side to demonstrate its effect on the simulated TCE degradation profile. As anticipated, the lower Henry's law constants caused increase the dechlorination rate slightly because more TCE is present in the liquid phase. Conversely, increasing the partitioning of TCE to the second phase greatly lowers the observed rate.

*4.5.3. Observed and intrinsic kinetics*

The partitioning of products into the gas phases reduces their observed degradation rate compared to the intrinsic kinetics of the system and thus it is of interest to observe the aqueous phase concentrations. For proper design of the remedial system using such an option, the knowledge of aqueous phase concentration is critical. Fig. 5a and b illustrate this effect for ratios of the gas to liquid phase of $V_g/V_w = 0.6$ and $V_g/V_w = 0$, respectively. One can see from the figure that the intermediates concentrations in the aqueous phase is a strong function of headspace volume. The degradation produces notably higher amount of intermediates in the case of zero-headspace system as compared to the headspace system. This is also evident from the Eq. (14). In the case of zero-headspace system, the apparent or observed rate constant reduces to the intrinsic value and hence we observe much greater production of intermediates.

Results reported in the literature thus far illustrate the effectiveness of the process considering observed rate constants. Fig. 5a and b show that for optimum design of the remediation systems, intrinsic rate constants should be used in lieu of observed rate constants. Different ways to improve the efficiency of the process should also be based on the intrinsic rate constants rather than the observed rate constants.

*4.5.4. Assessing the performance of the system*

This section illustrates how such a model can be used to study and improve the performance of the system. In the example illustrated, the primary non-toxic end product desired is ethene. As we recall from the reaction scheme (Fig. 1), ethene can be formed from 1,1-DCE, vinyl chloride and acetylene. Furthermore, acetylene production takes place through the complex Ethynylcobalamin, which is always present in the aqueous phase. With all the assumptions involved, this modeling analysis suggests that the current selectivity for complex formation is 43%, whereas that for *cis*-1,2-DCE is 54%. These are the main daughter products of TCE degradation which further react to give other intermediate species. From the reaction scheme, it is apparent that 1,1-DCE, which directly yields ethene would be the ideal candidate for which selectivity could be improved. However, 1,1-DCE has the lowest solubility in water (at 25°C) [20] among the three DCE isomers. It also has the highest Henry's law constant among the DCE isomers. Moreover, 1,1-DCE also has the most stringent drinking water standards and hence it is the least desirable. Between *cis*-1,2-DCE and *trans*-1,2-DCE, *trans*-1,2-DCE has an order of magnitude higher rate constant than that of *cis*-1,2-DCE. Hence it would be prudent to develop an electron mediator which would change the selectivity of TCE immediate daughter products to *trans*-1,2-DCE.

The above discussion is based on the different assumptions invoked while simulating the example problem. In few cases, some of these assumptions could be violated, and

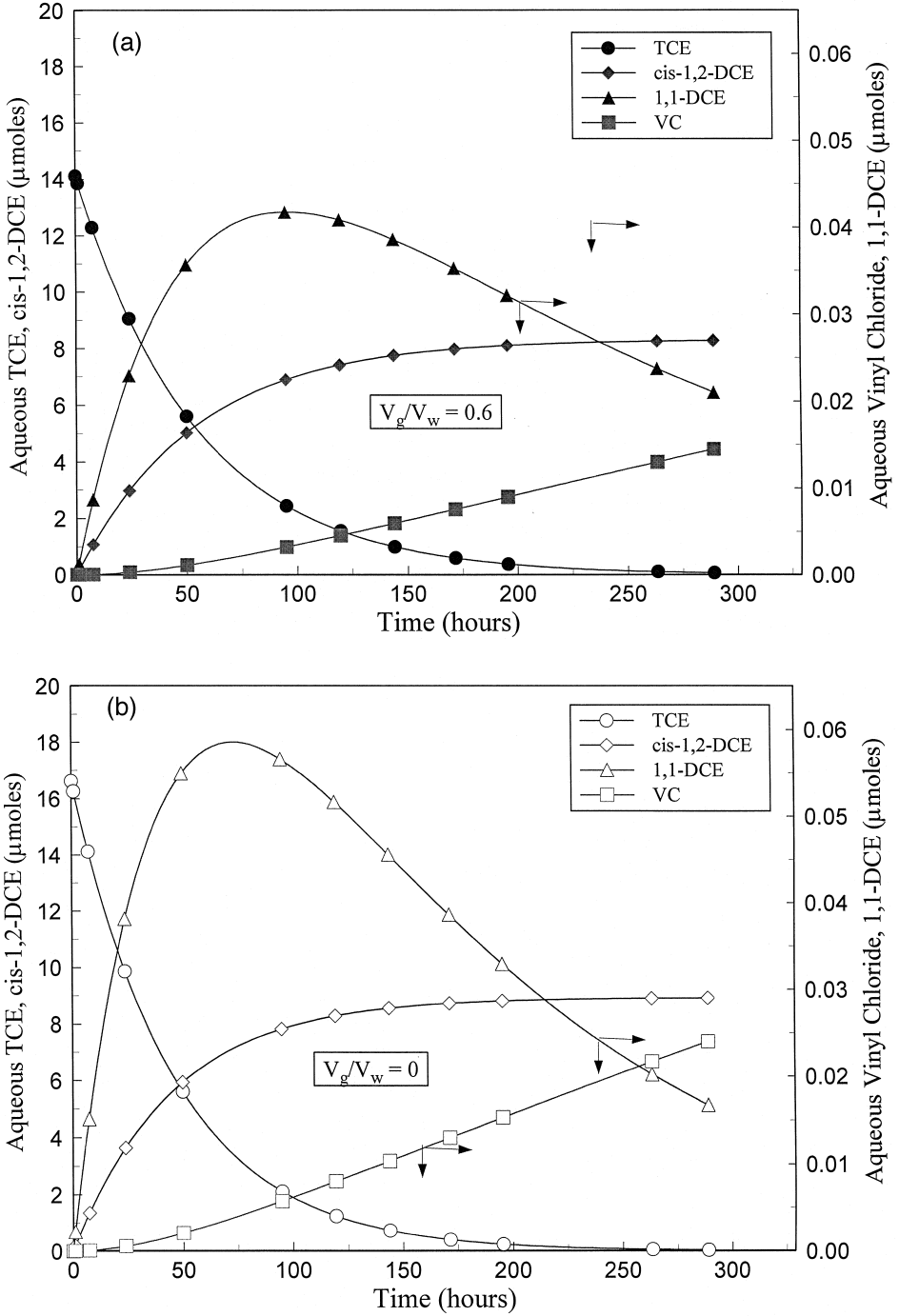


Fig. 5. Simulated product distribution in the aqueous phase (a) $V_g / V_w = 0.6$, (b) $V_g / V_w = 0$.

the modeling outcome could be different. Nevertheless, it illustrates different ways to analyze the system behavior without going into intricate experimental details, which often is very time consuming. In this respect, such a model is superior to the conventional trial and error experimental approach to arrive at optimum design, and can save large amount of efforts and experimental costs.

## 5. Example 2: reductive dehalogenation using zero-valent iron

It should be noted that the general model given by Eqs. (5) and (9) could be applied to any class of reaction involving two-phase system involving reaction and mass transfer of reactants and products between phases. However, each specific system would require a different set of mass balance equations. We expect to change the kinetic mechanisms and constants, mass transfer coefficients, partition models, and partition coefficients for each case. In this section, we apply the general principles used earlier in the development of model to the system of reductive dehalogenation of TCE using zero-valent iron data from our laboratory.

### *5.1. Experimental*

Batch runs were carried out in the laboratory for the degradation of TCE using zero-valent iron. Known amount of 40-mesh electrolytic iron powder (obtained from Fisher Scientific) was added to 40-ml glass hypovials. The hypovials were then filled with TCE solution of known concentration in deionized water, leaving no headspace and were sealed immediately with caps containing Teflon-lined septa. In order to simulate deoxygenated conditions, sodium bisulfite was added to the hypovials before sealing. The hypovials were then placed in an incubator shaker (150 rpm) allowing for complete mixing. At different times, a set of two hypovials was removed from the shaker and subsamples were transferred to vials for analysis. The detailed description about the experimental procedure and analytical method used has been reported in our previous paper [13].

### *5.2. Adaptation of mathematical model for the experimental system*

In Section 4, we have shown how the model (Eqs. (5) and (9)) can be altered to suit the gas–liquid system with reaction in liquid phase and mass transfer across gas–liquid interface. The experimental system employed here is a zero-headspace system. Hence, there is no gas–liquid mass transfer involved. However, due to the presence of solids (iron), adsorption/sorption phenomenon needs to be considered. Sorption of TCE on iron particles has been reported in literature [24]. It was observed that TCE sorption occurs at two sites—reactive and non-reactive sites, and the majority of this sorption is on the non-reactive sites. Further, this group of researchers has shown that the adsorption of TCE to iron follows the modified Langmuir type isotherm given by:

$$C^{s}_{TCE} = \frac{kb\left(C^{w}_{TCE}\right)^{M}}{1 + k\left(C^{w}_{TCE}\right)^{M}} \tag{15}$$

where $C^{s}_{TCE}$ and $C^{w}_{TCE}$ are the sorbed concentration (nmol/g) and aqueous concentration (nmol/ml), respectively. $M$, $k$, and $b$ are generalized Langmuir coefficients. The values of generalized Langmuir coefficients (with 40-mesh Fe system) were taken from literature [24]. The summary of these model parameters along with the experimental conditions used to verify the model is given in Table 3. With the iron and TCE system, it is reported [24] that the equilibrium sorption is achieved relatively fast (within 2 h) compared to the slow rate of reaction. It was postulated that the iron sorbed to the non-reactive sites cannot leave the surface and there is continuous regeneration of reactive sites as the TCE degrades. We can thus consider two steps again, degradation due to reaction and mass transfer (sorption) to these active sites. Therefore, the balance for the solid phase (Fe) concentration of TCE can be written as:

$$\frac{dC^{s}_{TCE} m_{Fe}}{dt} = -k_{intrinsic} C^{s*}_{TCE} m_{Fe} - (k_L a) V_w (C^{w}_{TCE} - C^{s}_{TCE}) \quad (16)$$

where $m_{Fe}$ is the amount of iron in grams. $k_{intrinsic}$ ($h^{-1}$) is the intrinsic degradation rate constant of TCE for the reaction at the surface of zero-valent iron and $k_L$ is the mass transfer coefficient from bulk liquid to solid (m/h). $a$ is the effective mass transfer area (solid/liquid interphase, $1/m$). For the simplification purposes, the rate of reaction on the surface of iron was assumed to be first order with respect to the concentration of TCE on the reactive sorption sites, $C^{s*}_{TCE}$. The first order rate expression with respect to aqueous phase concentration of TCE is well-documented in the literature. It should be noted that $C^{s*}_{TCE}$ is the concentration of TCE at the active reactive sites, whereas $C^{s}_{TCE}$ is the total concentration of TCE on the iron surface (as the sorption takes place at both reactive as well as non-reactive sites). To date, no study has been reported in the literature providing insight into the actual intrinsic degradation constant value at the iron surface, $k_{intrinsic}$. Major reason for this data gap is the analytical difficulties involved in the experimental system. Without prior knowledge of $k_{intrinsic}$ and the number of reactive sites, above equation would be very difficult to solve. Therefore, in the discussion that follows, we have simplified the analysis by assuming the equilibrium

Table 3
Model parameters used for zero-valent iron system

| Parameter | Value |
|---|---|
| Initial TCE concentration[a] | 80 mg/l (0.61 mM) |
| Amount of Iron (40-mesh) used[a] ($m_{Fe}$) | 10 gm |
| Volume of aqueous phase[a] ($V_w$) | 40 ml |
| $k^{c}_{TCE}$ | 0.0093[c]/h |
| $b$[b] | 882 |
| $k$[b] | 0.0207 |
| $M$[b] | 0.655 |

[a] Experimental conditions.
[b] Obtained from Ref. [24] (for $C^{w}$ and $C^{s}$ units of nmole/ml and nmole/g, respectively).
[c] Value obtained by fitting observed aqueous phase TCE concentrations to exponential fit.

between solid and liquid phases, and introducing a new parameter $A_s$, called as the 'fractional active site concentration', defined as:

$$A_s = \frac{C^{s*}_{TCE}}{C^{s}_{TCE}} \tag{17}$$

We also assume that there is quasi-equilibrium between the concentration in the liquid and solid surface. Using this assumption, Eq. (16) can be written as:

$$\frac{d\left(C^{s}_{TCE} m_{Fe}\right)}{dt} = -k_{intrinsic} A_s C^{s}_{TCE} m_{Fe} - \frac{V_w dC^{W}_{TCE}}{dt} \tag{18}$$

making use of Eq. (15), the above equation can be written in the form of aqueous phase concentrations as:

$$\frac{dC^{w}_{TCE}}{dt} = -\frac{\dfrac{kb\left(C^{w}_{TCE}\right)^{M}}{1+k\left(C^{w}_{TCE}\right)^{M}} k_{intrinsic} A_s m_{Fe}}{V_w\left[1+\dfrac{\left(m_{Fe} Mkb\left(C^{w}_{TCE}\right)^{M-1}\right)}{\left(V_w\left(1+k\left(C^{w}_{TCE}\right)^{M}\right)^{2}\right)}\right]} \tag{19}$$

### 5.3. Results and discussion

Eq. (19) was solved by numerical integration with the initial conditions and parameters given in Table 3. One can see that there are two unknown constants here—the intrinsic rate constant $k_{intrinsic}$, and the fractional active site concentration $A_s$. As anticipated, there were sets of these values for which the model concentrations matched the experimental values. The sum of least square errors between experimental and predicted concentrations was calculated for each such set. The surface plot of the error vs. $k_{intrinsic}$, and $A_s$ is shown as an inset in Fig. 6. One can see that the error reaches minima at several values of $k_{intrinsic}$ and $A_s$. It is interesting to note that, when the error is plotted against the product of $k_{intrinsic}$ and $A_s$ (Fig. 6), only one single minimum value was obtained. Thus, for a given iron surface (if the proper characterization techniques are available), using such error analysis one can find the intrinsic rate constant on the surface of the iron. One should be careful in carrying out such analysis, because the same product value can be obtained with different sets of $k_{intrinsic}$ and $A_s$ values, although we have some limits on both these parameters. $A_s$, i.e. the fractional active site concentration can vary between 0 and 1. The observed rate constant $k_{obs}$, obtained by exponential fit of aqueous phase TCE concentrations, is a lumped parameter which takes into account all the processes taking place on the surface of the iron and in the bulk of the liquid. Because of various diffusion processes taking place in the bulk liquid and on the surface of iron, this value will be lower than the actual intrinsic value. Indeed, we observed that even with $A_s = 1$, i.e., the entire surface of iron being assumed reactive, the value of intrinsic rate constant obtained ($\sim 0.1\ h^{-1}$) was almost an order of

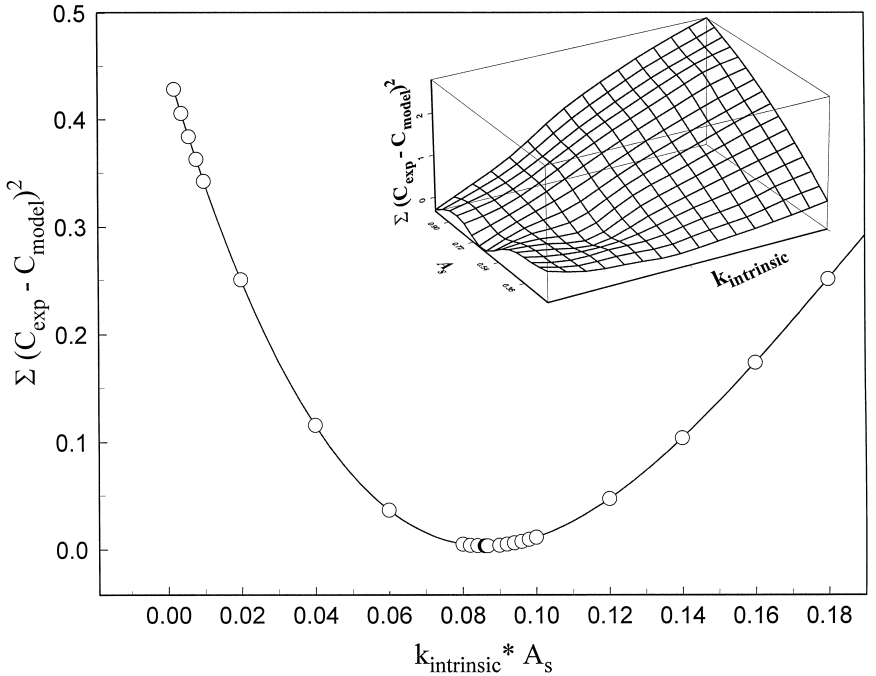


Fig. 6. Error analysis between experimental and predicted concentrations in case of reductive dehalogenation of TCE by zero-valent iron in zero-headspace system (inset: surface plot of least square error against $k_{intrinsic}$ and $A_s$).

magnitude higher than $k_{obs}$. The comparison between predicted and experimental concentration profiles for minimum error point is shown in Fig. 7.

It is interesting to note that the overall concentration profile predicted by Eq. (19), resembles the exponential profile, typical of the first order reactions. Thus, the overall effect of all these adsorption, reaction processes is a pseudo-first order process, which is well-observed in the literature. The reason for this will become clearer if we analyze different terms in the Eq. (19) in terms of order of magnitudes. It can be seen that at low values of concentrations, the term $kC_{TCE}^{w}$, will be negligible compared to 1 (as $k = 0.0207$). Hence, for lower values of $C$:

$$1 + kC_{TCE}^{w} \cong 1 \tag{20}$$

Further, as $M < 1$, we can see that:

$$1 + \frac{\left(m_{Fe} Mkb\left(C_{TCE}^{w}\right)^{M-1}\right)}{\left(V_w\left(1 + k\left(C_{TCE}^{w}\right)^{M}\right)^2\right)} \cong 1 + \frac{\left(m_{Fe} Mkb\left(C_{TCE}^{w}\right)^{M-1}\right)}{V_w} \tag{21}$$

using $M$, $k$, $b$, and $m_{Fe}$ from Table 3, this becomes:

$$1 + \frac{\left(m_{Fe} Mkb\left(C_{TCE}^{w}\right)^{M-1}\right)}{V_w} \cong 1 + 3\left(C_{TCE}^{w}\right)^{M-1} \cong 3\left(C_{TCE}^{w}\right)^{M-1} \tag{22}$$

Thus, Eq. (19) can be simplified to:

$$\frac{dC_{TCE}^{w}}{dt} = -\frac{kb\left(C_{TCE}^{w}\right)^{M} k_{intrinsic} A_s m_{Fe}}{3V_w\left(C_{TCE}^{w}\right)^{M-1}} = k'\left(C_{TCE}^{w}\right) \quad (23)$$

Thus, at lower values of concentration, the overall degradation process resembles the first order process. It can be seen from Fig. 7 that the agreement between the experimental and modeling values is excellent at earlier times. However, at longer times, the model predicts higher degree of degradation than that observed. The fact that the model predicted degradation is higher than the experimental observation is further illustrated by comparison of values of apparent pseudo-first order degradation constants. The observed degradation constant reported for this particular experimental set up is 0.0093 $h^{-1}$ [13] (value found by regressing the observed aqueous phase concentrations to first order decay expression). From Eq. (23), the calculated value of apparent degradation constant ($k'$) obtained is 0.0114 $h^{-1}$. The difference between the two can be explained as follows. In the analysis, we have assumed the value of $A_s$ to be constant throughout the course of experiment. But as the reaction proceeds, due to effects such as pH change, etc., various precipitates (such as siderite, iron hydroxide) could be formed on the surface of iron, and this would in turn change the morphology of the iron surface. Thus, as the time progresses, $A_s$ decreases owing to formation of these precipitates. Consequently, we observe lower rates of degradation. In addition, other factors such as migration of TCE from nonreactive to reactive sites need to be considered.

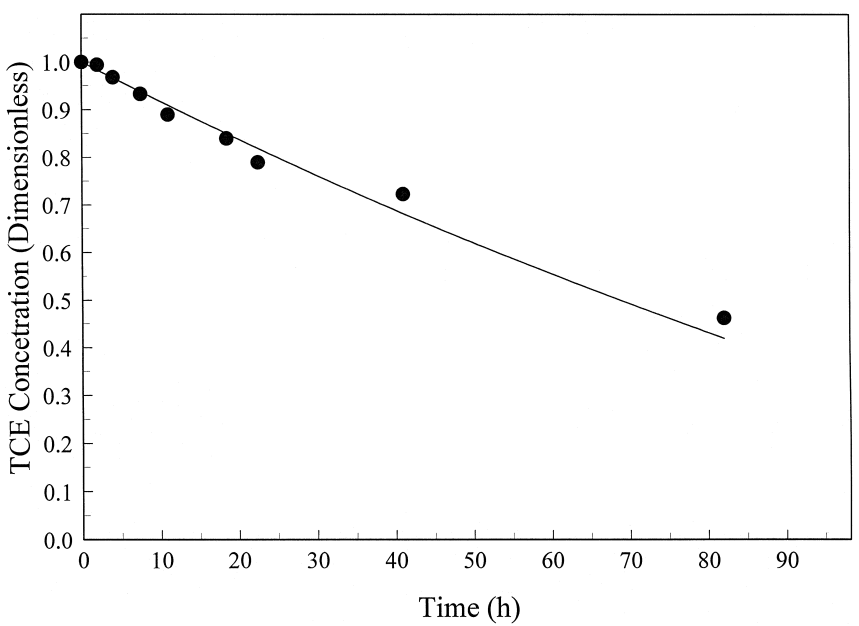


Fig. 7. Reductive dehalogenation of TCE by zero-valent iron in zero headspace system. Symbols: experimental (initial TCE 80 mg/l, iron: 40 mesh, 10 gm, $V_w$ = 40 ml) Line: prediction of model accounting for sorption.

We are currently in the process of incorporating the variation of $A_s$ with time in the model.

## 6. Summary and conclusions

A two-phase kinetic model has been developed for the general class of reactions involving reaction in one phase and mass transfer between two phases. The model has been applied to the system of reductive dehalogenation of trichloroethylene. The model predictions have been verified experimentally from literature results and our experimental data for two different systems involving reductive dehalogenation of trichloroethylene. In the case of vitamin $B_{12}$, the model predicts the degradation process quite accurately over the entire time range, for most of the intermediates. With zero-valent iron, we have illustrated how the sorption phenomena can be readily incorporated into the model. A new concept of fractional active site concentration is introduced to incorporate the differences in the sorption. The model also conforms with the observed pseudo first order behavior of the system. To the best of our knowledge, this is the first systematic effort to carry out the kinetic analysis of the reductive dehalogenation of TCE. Using the example of trichloroethylene, it is shown how model can also be used to arrive at future research directions in order to improve the overall effectiveness of the process. Furthermore, such models can be combined with traditional transport theories to determine monitoring protocols and evaluate remediation alternatives for specific contaminated sites.

## 7. Nomenclature

| | |
|---|---|
| $a$ | interfacial area per unit volume of solution ($m^{-1}$) |
| $A_s$ | fractional active site concentration |
| $b$ | Langmuir adsorption isotherm parameter |
| $C_0$ | initial concentration of TCE in aqueous phase (mol/l) |
| $C_i^g$ | concentration of component $i$ in gaseous phase (mol/l) |
| $C_i^w$ | concentration of component $i$ in aqueous phase (mol/l) |
| $C_{TCE}^{s*}$ | concentration of TCE at reactive sites (nmol/g) |
| $C_{TCE}^{s}$ | total concentration of TCE on the iron surface (nmol/g) |
| $C_{TCE}^{w}$ | concentration of TCE in aqueous solution (nmol/ml) |
| $k$ | Langmuir adsorption isotherm parameter |
| $k'$ | predicted apparent degradation constant ($h^{-1}$) |
| $k_{AC}$ | degradation rate constant for acetylene ($h^{-1}$) |
| $k_{1,1\text{-DCE}}$ | degradation rate constant for 1,1-DCE ($h^{-1}$) |
| $k_{cis\text{-DCE}}$ | degradation rate constant for *cis*-DCE ($h^{-1}$) |
| $k_{trans\text{-DCE}}$ | degradation rate constant for *trans*-DCE ($h^{-1}$) |
| $k_{ET}$ | degradation rate constant for ethene ($h^{-1}$) |
| $k_{g,i}$ | mass transfer coefficient for component $i$ (m/h) |
| $k_{H,i}$ | Henry's Law constant for component $i$ (Pa $m^3$/mol) |

| | |
|---|---|
| $k_i^{app}$ | apparent degradation rate constant of species $i$ |
| $k_{intrinsic}$ | intrinsic TCE degradation constant on the iron surface |
| $k_L$ | liquid solid mass transfer coefficient for TCE between water and iron (m/s) |
| $k_{TCE}$ | degradation rate constant for TCE ($h^{-1}$) in vitamin $B_{12}$ system |
| $k_{TCE\text{-}complex}$ | rate constant for formation of complex Ethynylcobalamin from TCE |
| $k_{TCE\text{-}1,1\text{-}DCE}$ | rate constant for formation of 1,1-DCE from TCE |
| $k_{TCE\text{-}cis\text{-}DCE}$ | rate constant for formation of *cis*-1,2-DCE from TCE |
| $k_{TCE\text{-}trans\text{-}DCE}$ | rate constant for formation of *trans*-1,2-DCE from TCE |
| $k_{TCE\text{-}VC}$ | rate constant for formation of VC from TCE |
| $k_{VC}$ | degradation rate constant for vinyl chloride ($h^{-1}$) |
| $M$ | Langmuir adsorption isotherm parameter |
| $m_{Fe}$ | amount of iron (g) |
| $V_g$ | volume of gas phase (l) |
| $V_w$ | volume of aqueous phase (l) |

*Chemicals abbreviations*

| | |
|---|---|
| AC | Acetylene |
| DCE | Dichloroethylene |
| ET | Ethylene |
| TCE | Trichloroethylene |
| VC | Vinyl chloride |

## Acknowledgements

This work was partially supported by a Memorandum of Agreement between Kentucky Natural Resources and Environmental Protection Cabinet and the University of Kentucky through the Kentucky Water Resources Research Institute. Authors would also like to thank Dr. David Burris for providing the raw experimental data and comments.

## References

[1] R.J. McKinnon, J.E. Dyksen, Removing organics from groundwater through aeration plus GAC, Journal AWWA, 1984, pp. 42–47.

[2] R.L. Gross, S.G. Termath, Packed tower aeration strips TCE from groundwater, Environ. Prog. 4 (1985) 119–124.

[3] W.H. Glaze, J.-W. Kang, Advanced oxidation processes for treating groundwater contaminated with TCE and PCE: laboratory studies, Journal AWWA, 1988, pp. 57–63.

[4] P.M.L. Bonin, M.S. Odziemkowski, R.W. Gillham, Impact of chlorinated solvents on polarization and corrosion behavior of iron electrodes with respect to their reductive dechlorination by iron, American Chemical Society, Division of Environmental Chemistry Extended Abstracts, Vol. 37 (1), 1997, pp. 86–88.

[5] T. Boronina, K.J. Klabunde, G. Sergeev, Destruction of organohalides in water using metal particles: carbon tetrachloride/water reactions with magnesium, tin, and zinc, Environ. Sci. Technol. 29 (6) (1995) 1511–1517.
[6] B. Deng, T.J. Campbell, D.R. Burris, Kinetics of vinyl chloride reduction by metallic iron in zero-headspace systems, American Chemical Society, Division of Environmental Chemistry Extended Abstracts, Vol. 37 (1), 1997, pp. 81–83.
[7] M.M. Scherer, J.C. Westall, P.G. Tratnyek, Kinetics of carbon tetrachloride reduction at an iron rotating disk electrode, American Chemical Society, Division of Environmental Chemistry Extended Abstracts, Vol. 37 (1), 1997, pp. 85–86.
[8] T.M. Sivavec, D.P. Horney, Reduction of chlorinated solvents by Fe(II) minerals, American Chemical Society, Division of Environmental Chemistry Extended Abstracts, Vol. 37 (1), 1997, pp. 115–117.
[9] T.M. Sivavec, P.D. Mackenzie, D.P. Horney, Effect of site groundwater on reactivity of bimetallic media: deactivation of nickel plated granular iron, American Chemical Society, Division of Environmental Chemistry Extended Abstracts, Vol. 37 (1), 1997, pp. 83–85.
[10] W.-X. Zhang, C.-B. Wang, Rapid and complete dechlorination of TCE and PCBs by nanoscale Fe and Pd/Fe particles, American Chemical Society, Division of Environmental Chemistry Extended Abstracts, Vol. 37 (1), 1997, pp. 78–79.
[11] G.D. Sayles, G. You, M. Wang, M.J. Kupferle, DDT, DDD, and DDE dechlorination by zero-valent iron, Environ. Sci. Technol. 31 (12) (1997) 3448–3454.
[12] L.J. Matheson, P.G. Tratnyek, Reductive dehalogenation of chlorinated methanes by iron metal, Environ. Sci. Technol. 28 (6) (1994) 2045–2053.
[13] J. Gotpagar, E. Grulke, T. Tsang, D. Bhattacharyya, Reductive dehalogenation of trichloroethylene using zero-valent iron, Environmental Progress 16 (2) (1997) 137–143.
[14] D.R. Burris, C.A. Delcomyn, M.H. Smith, A.L. Roberts, Reductive dechlorination of tetrachloroethylene and trichloroethylene catalyzed by vitamin $B_{12}$ in homogeneous and heterogeneous systems, Environ. Sci. Technol. 30 (10) (1996) 3047–3052.
[15] R.W. Gillham, S.F. O'Hannesin, Enhanced degradation of halogenated aliphatics by zero-valent iron, Ground Water 32 (4) (1994) 958–967.
[16] A.L. Roberts, L.A. Totten, W.A. Arnold, D.R. Burris, T.J. Campbell, Reductive elimination of chlorinated ethylenes by zero-valent metals, Environ. Sci. Technol. 30 (8) (1996) 2654–2659.
[17] G. Glod, W. Angst, C. Holliger, R.P. Schwarzenbach, Corrinoid mediated reduction of tetrachloroethene, trichloroethene, and trichlorofluroethene in homogeneous aqueous solution: reaction kinetics and reaction mechanisms, Environ. Sci. Technol. 31 (1) (1997) 253–260.
[18] M. Semadeni, P. Chiu, M. Reinhard, The reductive transformation of chlorinated ethenes, chloroacetylene and acetylene catalyzed by vitamin $B_{12}$, American Chemical Society, Division of Environmental Chemistry Extended Abstracts, Vol. 37 (1), 1997, pp. 123–125.
[19] G. Glod, U. Brodmann, W. Angst, C. Holliger, R.P. Schwarzenbach, Cobalamin-mediated reduction of *cis*- and *trans*-dichloroethylene, 1,1-dichloroethene, and vinyl chloride in homogeneous aqueous solution: reaction kinetics and mechanistic considerations, Environ. Sci. Technol. 31 (11) (1997) 3154–3160.
[20] P.V. Roberts, P.G. Dandliker, Mass transfer of volatile organic contaminants from aqueous solution to the atmosphere during surface aeration, Environ. Sci. Technol. 17 (8) (1983) 484–489.
[21] D. Mackay, W.Y. Shiu, K.C. Ma, Illustrated Handbook of Physical Chemical Properties and Environmental Fate for Organic Chemicals, Vol. III, 1992, p. 493.
[22] D. Mackay, W.Y. Shiu, Critical review of Henry's law constants for chemicals of environmental interest, J. Phys. Chem. Ref. Data 10 (4) (1981) 1175–1199.
[23] J.M. Gossett, Measurement of Henry's law constants for $C_1$ and $C_2$ chlorinated hydrocarbons, Environ. Sci. Technol. 21 (1987) 202–208.
[24] D.R. Burris, T.J. Campbell, V.S. Manoranjan, Sorption of trichloroethylene and tetrachloroethylene in a batch reactive metallic iron–water system, Environ. Sci. Technol. 29 (11) (1995) 2850–2855.